Check for updates

Suitability of the SWAT Model for Simulating Water Discharge and Sediment Load in a Karst Watershed of the Semiarid Mediterranean Basin

Alberto Martínez-Salvador [1] · Carmelo Conesa-García [2] (iD)

Abstract

This paper presents a case study conducted in the Upper Argos River, in southeast Spain, to verify the applicability of the SWAT model for prediction of the water discharge and sediment load in a Mediterranean semiarid karst basin. For this purpose, the monthly and yearly discharge and sediment load records at the Argos reservoir gauge during the period 1976–2000 were used to calibrate the model, while data from 2001 to 2017 were used for validation. For both stages of the modeling the performance of the NSE, RSR, and PBIAS indices was good in the case of the monthly flow rate (NSE = 0.62 and 0.70 for calibration and validation, respectively; RSR = 0.61 and 0.54; PBIAS = −20.60% and − 16.09%) and acceptable for the estimation of the monthly sediment load (NSE = 0.52 and 0.58; RSR = 0.70 and 0.64; PBIAS = 10.65% and 15.20%). These indices showed a substantial improvement in the annual simulations, particularly in the calibration, for which the respective values of NSE and RSR were 0.89 and 0.32 for the flow rate and 0.81 and 0.42 for the sediment transport.

✉ Carmelo Conesa-García
cconesa@um.es

Alberto Martínez-Salvador
https://orcid.org/0000–0002-9113–3487

[1] Research Group on Erosion and Desertification in Mediterranean Environments, University of Murcia, Campus de La Merced, 30001 Murcia, Spain

[2] Department of Physical Geography, University of Murcia, Campus de La Merced, 30001 Murcia, Spain

1 Introduction

The SWAT (Soil and Water Assessment Tool) model has had extensive recognition among the members of the scientific community dedicated to hydrological modeling (Moriasi et al. 2007; Gassman et al. 2007; Arabi et al. 2008). Its ability to analyze hydrological processes and the possibility of its application to very different environmental scenarios have generated an extensive literature on this subject (Gassman et al. 2007).

Most studies involving the SWAT model have focused on the assessment of the potential impacts of climate change and land use on water flow and sediment load for a large variety of regions and watershed scales (Kiros et al. 2015; Nerantzaki et al. 2015; Luan et al. 2018). This wide range of environmental conditions and spatio-temporal scales often generates uncertainty. The best predictions are achieved in monitored basins with gauging stations, whose data serve to calibrate and validate the model developed. In such cases, it is usually observed that SWAT offers a better fit for long-term simulations (monthly, seasonal, and yearly) and that daily discharges are poorly predicted (Kiros et al. 2015).

The uncertainty increases significantly in ungauged basins or when there are few flow measurement points. In particular, in arid and semiarid areas, drained by non-continuous flows, a careful analysis of sensitivity and calibration is required (Yesuf et al. 2016).The watershed in these areas is characterized by prolonged periods of drought and high evaporation, isolated torrential rainfall events causing flash floods, low base flows or dry streams most of the year, and flow transmission losses through the channel bed. This explains why there are fewer examples of SWAT application under these conditions, and the studies performed in semiarid areas (e.g., Molina-Navarro et al. 2014; Yuan et al. 2014; Kiros et al. 2015; Zettam et al. 2017; Brouziyne et al. 2017; Ahn et al. 2018; Santos et al. 2018) agree on the need to carry out an adequate calibration of the model, according to the most sensitive parameters that control the hydrological response and its optimum range in such environments. In particular, Yuan et al. (2014) analyzed the influence of extreme hydrological events in Arizona watersheds, and found that the PBIAS ranged from −25 to +25% in uncalibrated modeling.

The degree of uncertainty increases when a basin is simultaneously subject to semiarid climatic conditions and the effects of hydrological regulation exerted by karstic terrain. It is then necessary to introduce a greater number of parameters in the model or to modify certain algorithms, making the calibration complex. Another factor of uncertainty arises from the lengths of the calibration and validation periods. These periods were less than 5 years in numerous studies that applied SWAT (e.g., Nikolaidis et al. 2013; Ahn et al. 2018; Brouziyne et al. 2018; Chen et al. 2018), but in a few cases they exceeded 10 years (Malagò et al. 2016; Santos et al. 2018).

The general objective of this study is to evaluate the efficiency of the SWAT model for the prediction of water and sediment discharges (monthly and yearly) in small semiarid Mediterranean basins with a karstic influence and for which long data series from gauging stations are available. Specifically, it has been applied to the watershed area of the Argos reservoir (basin of the Argos River, a tributary of the Segura River), which has a significant series of flow data and sufficient sediment gauges to perform calibration and validation of the values estimated. Particular attention has been paid to the identification of the most sensitive parameters of the model according to the environmental conditions of the basin, the analysis of the impact of the sensitive parameters on the hydrological response within each component of the simulation process, and the calibration of SWAT to determine the contribution of surface runoff and base flow.

2 Materials and Methods

2.1 Study Site

The Argos River basin is located in the southeastern Iberian Peninsula (in the northwest of the Region of Murcia) (Fig. 1). This area (510 km²) has an average altitude of 925 m, which masks the contrast between its headwater (maximum altitude of 1713 m) and the lower part (minimum altitude of 256 m). Mountainous headlands give way downstream to plains and undulating landforms, carved by ephemeral channels that converge in the Argos River. These relief forms, framed within the Baetic Cordilleras (Medium Subbetic domain), are the result of alpine orogeny and later tectonic activities (post-Pliocene), associated with a compressive stage that deformed the previous structures and created seismic focus, subvolcanic rock outcrops, and strike-slip faults (Navarro-Hervas and Rodríguez-Estrella 2001). In the northern and western parts there are limestone and dolomite outcrops from the Jurassic age, and in the southeastern and eastern parts clays of the Trias, while in the central part Neo-Quaternary formations of marls, limestones, and sandstones are more prevalent.

The Argos River basin has semiarid climatic features. The difference in altitude is reflected in the climatic conditions with an annual average precipitation of 345 to 440 mm, average monthly temperatures between 11 and 16 °C, an absolute maximum and minimum of 44 °C (August) and − 10 °C (February), respectively, and an average annual temperature of around 13 °C. Under such environmental conditions, very diverse soils have developed, among which calcic Xerosols predominate. The groundwater systems, and in particular the karst lands in the headwater areas, have a great regulatory effect on the flow in the Argos River, providing it with a hydrological regime that is less variable than that of many such rivers in Mediterranean semiarid environments.

2.2 SWAT Model

The SWAT model is a hydrological model based on physical, semi-distributed, and continuous simulation that is applied at the scale of the watershed (Arnold et al. 1998), for the estimation and simulation of the generation of flow and sediment yield in a basin (Neitsch et al. 2009).

The SWAT divides the watershed into a number of sub-basins, establishing Hydrological Response Units or HRUs, whose purpose is to effect all the possible combinations of three major input variables of the model: land use, lithology and slope. This provides a more realistic basin model, based on different HRUs for each sub-basin, allowing calculations to be performed with greater accuracy. The simulation of the hydrological cycle by the SWAT is based on the general equation of the water balance (Neitsch et al. 2009):

$$SW_t = SW_0 + \sum_{i=1}^{t} \left(R_{day} - Q_{surf} - E_a - W_{seed} - Q_{qw} \right) \qquad (1)$$

where SW_t is the final water content (mm), SW_0 is the initial water content (mm), t is the day, R_{day} is the amount of precipitation (mm), Q_{surf} is the amount of surface runoff (mm), W_{seed} is the amount of water accumulated in the unsaturated zone (mm), and Q_{qw} is the amount of return flow (mm) (Arnold et al. 2011).
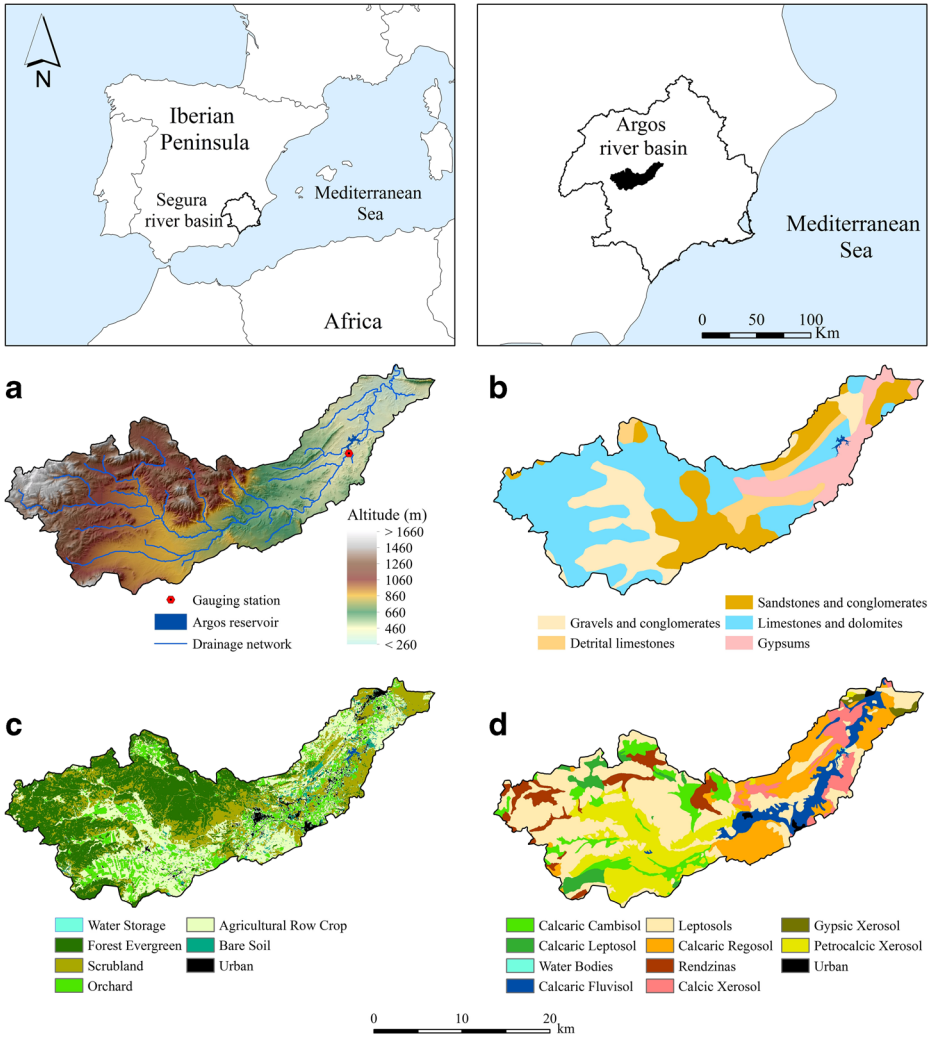
Fig. 1 The Argos catchment in southeast Spain: DTM (**a**), lithological map (**b**), land use (**c**), and soil types (**d**)

In the present study we used the SCS-CN method for the calculation of surface runoff according to the following equation:

$$Q_{surf} = \frac{\left(R_{day} - I_a\right)^2}{\left(R_{day} - I_a + I_a S\right)} \tag{2}$$

where R_{day} is the rainfall depth (mm), I_a is the initial abstraction related to surface storage, interception, and infiltration before the start of runoff (mm), and S is the retention parameter (mm).

The modified rational method (MRM) (Eq. (3)) is applied by the SWAT for the estimation of the maximum runoff flow rate in each rainfall event. This method has been integrated into

various methods that aim to predict sediment loss at the basin level. In particular, the SWAT model uses the MRM (Eq. 3) to calculate the maximum runoff peak.

$$Q_{peak} = \frac{C \cdot i \cdot A}{3.6} \tag{3}$$

where Q_{peak} is the peak runoff (m³/s), C is the runoff coefficient, i is the rainfall intensity (mm/h), A is the area of the sub-basin (km²), and 3.6 is an unit conversion factor to give m³/s.

For the calculation of sediment yield, the SWAT uses the MUSLE (Modified Universal Soil Loss Equation) (Williams and Brendt 1977), as follows:

$$Sed = 11.8 \left(Q_{surf} \cdot Q_{peak} \cdot area_{hru} \right)^{0.86} \cdot K_{USLE} \cdot C_{USLE} \cdot P_{USLE} \cdot LS_{USLE} \cdot CFRG \tag{4}$$

where Sed is the sediment yield (t), $area_{hru}$ is the area of the HRUs (ha), K_{USLE} is the erodibility factor, C_{USLE} is the management and land cover factor, P_{USLE} is the conservation practice factor, LS_{USLE} is the topographic factor, and $CFRG$ is the macro fragment factor.

The amount of sediment that is transported to the basin's drainage point is calculated from Eq. (5):

$$Sed_{OUT} = Sed_{IN} - Sed_{DP} + Dg_T \tag{5}$$

where Sed_{OUT} is the sediment transported in the basin (t), Sed_{IN} is the sediment generated in the whole basin (t), Sed_{DP} is the sediment that is deposited (t), and Dg_T is the total degradation of the basin (t).

The total degradation is obtained from the drag and erosion of the bed components, by the equation:

$$Dg_T = (D_r + D_B)(1 - D_R) \tag{6}$$

where D_r is the input sediment (t), D_B is the degradation of the bed material (t), and D_R is the sediment delivery ratio.

2.3 Inputs Data

The SWAT requires the entry of variables referring to terrain elevation and slope (DTM data), weather data to generate and simulate rainfall events, information about erodibility of soils (soil data) and vegetation cover (land use data), and finally hydrological and sediment data for model calibration and verification.

2.3.1 Digital Terrain Model (DTM)

A 20 m resolution DTM was obtained from LIDAR, using the ETRS89 / UTM zone 30 N (website of the IGN -Instituto Geográfico Nacional-). This resolution is considered suitable for the correct representation of the differentiating topographic features of the terrain in small-sized basins such as ours (Lin et al. 2010; Goyal et al. 2018).

2.3.2 Weather Data

The daily data of precipitation (mm), minimum temperature (°C), and maximum temperature (°C) used here correspond to 45 years (1973–2017) of records at the 7120E-Embalse del Argos station (Territorial Center of Meteorology of Murcia, AEMET). The rest of the climatic variables, such as daily wind speed, daily solar radiation (MJ/m²), and daily relative humidity (%), were obtained from the global database of the SWAT weather module.

2.3.3 Soil Data

Different physical and chemical properties of the soil were considered, using data provided by the project LUCDEME (Fight against Desertification in the Mediterranean), prepared by Alias and Ortiz (1986–2004) for the Region of Murcia (Fig. 1d). These included hydraulic conductivity, bulk density, organic matter content and depth of each edaphic horizon, as well as the percentages of clay, silt, and sand.

2.3.4 Land Use Data

The land use data were obtained from a LANDSAT 8 OLI image of 30 m resolution, captured on June 7, 2015 (Fig. 1c). After its radiometric correction, a multispectral improvement was made through the fusion of the high resolution panchromatic band and the low resolution bands by the Pan-Sharpening method, to which a supervised classification was applied, with high reliability in the results (Global Accuracy = 95.6% and Kappa Index = 0.95).

2.3.5 Hydrological Data

These were obtained from the gauging reports provided by CEDEX for the Segura watershed. As a starting point, we used the data series of the daily average flow (m³/s) of the entry into the Argos reservoir, corresponding to the period 1973–2017; that is, from the beginning of the exploitation of the reservoir until 2017. Since there is no flowmeter to measure the flow rate, the flow of the input was calculated from the balance between the reserve and the output of the previous day (Eq. (7)):

$$InR = (aR - dR) + S \tag{7}$$

where InR is the inflow to the reservoir (m³/s), aR is the current day's reserve (m³), dR is the previous day's reserve (m³), and S is the flow output of the previous day (m³/s).

The sediment transport information introduced refers to the average daily suspended and dissolved load at the entrance of the Argos River reservoir, for the period 1973–2017. These daily values were estimated by Martínez-Salvador and Conesa-García (2018), using log-linear regression models, from a total of 48 records of flow and sediment transport obtained in several surveys between 1983 and 1994 (CEDEX 1994).

2.4 Model Calibration and Validation

For the calibration and validation of the SWAT model, the series consisting of the years 1972–1975 was used as warm-up stage. In order to calibrate and validate the model, information relating

to the periods 1976–2000 and 2001–2017 respectively was handled. For the calibration phase, a sensitivity analysis was carried out with SWAT-CUP software, to detect the parameters in the model that were most influential and, therefore, most susceptible to modification.

For such purpose, this module offers different methods, including the SUFI-2 (Sequential Uncertainty Fitting) method, which was used here to perform the sensitivity analysis, calibration, and validation, because it requires a smaller number of interactions and a moderate processing time to obtain the best result. To pass to the validation stage, the model had to satisfy, in both simulations (flow and sediment transport), the requirements of RSR <0.70, NSE >0.50, and PBIAS between ±15 and ±25% (Moriasi et al. 2007) during the calibration. In the cases where these requirements were not achieved, the model was recalibrated, adding or deleting parameters as necessary in order to get them. The parameters used for the analysis of sensitivity in the estimation of flow and sediment load were selected on the basis of the SWAT documentation (Neitsch et al. 2009) and related literature (Arabi et al. 2008; Malagò et al. 2016).

The results were evaluated using six statistical methods, as recommended by Moriasi et al. (2007): 1) Nash-Sutcliffe efficiency (NSE) (Eq. (8)), 2) aggregation index (d) (Eq. (9)), 3) percent bias (PBIAS) (Eq. (10)), 4) root mean square error (RMSE) (Eq. (11)), 5) coefficient of determination (R^2) (Eq. (12)), and 6) standard deviation ratio (RSR) (Eq. (13)):

$$NSE = 1 - \left[\frac{\sum_{i=1}^{n} \left(Y_i^{obs} - Y_i^{sim} \right)^2}{\sum_{i=1}^{n} \left(Y_i^{obs} - Y_{obs}^{mean} \right)^2} \right] \tag{8}$$

$$d = 1 - \frac{\sum_{i=1}^{n} \left(Y_i^{obs} - Y_i^{sim} \right)^2}{\sum_{i=1}^{n} \left(Y_i^{sim} - \overline{Y_i^{sim}} \right) + Y_i^{obs} - \overline{Y_i^{obs}})^2} \tag{9}$$

$$PBIAS\ (\%) = \left[\frac{\sum_{i=1}^{n} \left(Y_i^{obs} - Y_i^{sim} \right) \cdot (100)}{\sum_{i=1}^{n} \left(Y_i^{obs} \right)} \right] \tag{10}$$

$$RMSE = \sqrt{\frac{\sum_{i=1}^{n} \left(Y_i^{obs} - Y_i^{sim} \right)^2}{n}} \tag{11}$$

$$R^2 = \frac{\left(\sum_{i=1}^{n} \left(Y_i^{obs} - Y_{obs}^{mean} \right) \left(Y_i^{sim} - Y_{sim}^{mean} \right) \right)^2}{\sum_{i=1}^{n} \left(Y_i^{obs} - Y_{obs}^{mean} \right)^2 \sum_{i=1}^{n} \left(Y_i^{sim} - Y_{sim}^{mean} \right)^2} \tag{12}$$

$$RSR = \frac{RMSE}{STDEV_{obs}} \tag{13}$$

where Y_i^{obs} is the i-th observation for the component that is being evaluated, Y_i^{sim} is the i-th simulation for the component that is being evaluated, Y_{obs}^{mean} is the mean of the observed data

for the component that is being evaluated, Y_{sim}^{mean} is the mean of the simulated data for the component that is being evaluated, $STDEV_{obs}$ is the standard deviation of the observed data, and n is the total number of observations. The degree of fit of the results, obtained from these statistics, was defined according to the interpretation and ranges established by Moriasi et al. (2007) (Table 1).

3 Results and Discussion

3.1 Sensitivity Analysis

The way in which the fit of the value of the parameter values affected the output of the model was evaluated in order to identify the parameters that could improve the characteristics of the model.

The sensitivity analysis determined that the most sensitive parameters for the flow prediction were: the hydraulic conductivity (CH_K2), the snow melt base temperature (SMTMP), the biological mixing efficiency (BIOMIX), the Manning's roughness (CH_N2), the groundwater revap coefficient (GW_REVAP), the snowfall temperature (SFTMP), the soil available water capacity for the first layer (SOL_AWC), the surface runoff lag time (SURLAG), the deep aquifer percolation coefficient (RCHRG_DP), the effective hydraulic conductivity in the tributary channel alluvium (CH_K1), the soil evaporation compensation factor (ESCO), and the Curve number (CN2) (Table 2).

The high sensitivity of the parameters CH_K2, GW_REVAP, RCHRG_DP, and CH_K1 revealed the importance of the aquifer system and groundwater dynamics in the hydrological regime. The infiltration in the soil profile, the transmission losses, and the percolation of the water to the deep aquifer were accounted for through the adjustment of the recharge parameter of the deep aquifer (RCHRG_DP), calibrating in turn the revap coefficient of the groundwater. The sensitive parameters identified in this study are consistent with those found in other, recent studies (Schmalz and Fohrer 2009; Betrie et al. 2011; Asl-Rousta et al. 2018; Chen et al. 2018).

The sensitivity of ESCO is also important because it is related to the high rate of evapotranspiration that occurs in this type of area. Similar results were found in other watersheds in the Mediterranean basin, under semiarid climatic conditions (Molina-Navarro et al. 2014; Brouziyne et al. 2017; Luan et al. 2018).

The most sensitive parameters in the erosion simulation were the Curve number (CN2), which was readjusted, the linear parameter for the sediment re-entrained in the channel (SPCON), and the average slope length (SLSUBBSN) (Table 3).

Table 1 Evaluation metrics and associated performance ratings

Performance Rating	RSR	R^2	d	NS	PBIAS (%)	
					Streamflow	Sediment
Verygood	0.0–0.5	0.75–1.00	0.75–1.00	0.75–1.00	<±10	<±15
Good	0.5–0-6	0.65–0.75	0.65–0.75	0.65–0.75	±10 - ±15	±15 - ±30
Satisfactory	0.6–0.7	0.50–0.65	0.50–0.65	0.50–0.65	±15 - ±25	±30 - ±35
Unsatisfactory	> 0.7	≤ 0.5	≤ 0.5	≤ 0.5	≥ ± 25	≥ ± 55

Table 2 Ranking of the most influential parameters in the simulation of flow

Parameter	Rank	P Value	t-Stat	Initial range	Default value	Fitted value
CH_K2.rte	1	0.00	66.8	0.01–500	5.00	0.03
SMTMP.bsn	2	0.00	7.71	−20 - 20	0.50	13.90
BIOMIX.mgt	3	0.00	6.23	0.0–1.0	0.30	10.81
CH_N2.rte	4	0.00	5.66	0.01–0.3	0.014	0.07
GW_REVAP.gw	5	0.00	5.27	0.02–0.2	0.02	−0.09
SFTMP.bsn	6	0.00	4.71	−20 - 20	1.00	20.03
SOL_AWC(1).sol	7	0.00	3.49	0.0–1.0	0.13	0.13
SURLAG.bsn	8	0.00	−3.30	0.05–24	4.00	6.01
RCHRG_DP.gw	9	0.00	−3.33	0–1	0.05	−0.82
ESCO.hru	10	0.00	−4.20	0–1	1.00	1.00
CH_K1.sub	11	0.00	−5.24	0–300	15.0	242.24
CN2.mgt	12	0.00	−6.25	0–100	74.0	0.26
GWQMN.gw	13	0.01	2.58	0–5000	500	15.54
EPCO.hru	14	0.02	−2.42	0–1	0.95	0.41
SOL_CRK.sol	15	0.03	2.12	0–1	0.10	0.67
ANION_EXCL.sol	16	0.05	1.94	0.01–1	0.02	0.17
SOL_K(1).sol	17	0.06	−1.86	0–2000	1.29	−1.71
SOL_BD(1).sol	18	0.11	1.60	0.9–2.5	1.34	0.03
ADJ_PKR.bsn	19	0.11	1.59	0.5–2	1.00	2.23
EVLAI.bsn	20	0.13	1.53	0–10	3.00	1.88
GW_SPYLD.gw	21	0.16	−1.41	0–0.4	0.10	0.89
LAT_TTIME.hru	22	0.28	1.07	0–180	0.00	95.93
CH_N1.sub	23	0.35	−0.94	0.01–30	0.014	17.10
ALPHA_BNK.rte	24	0.57	−0.57	0–1	0.30	1.29
REVAPMN.gw	25	0.87	0.17	0–500	10.0	7.09

Following the recommendations of Arabi et al. (2008), three parameters that define the protection of the cultivation terraces were included: the curve number (CN2), the average slope length (SLSUBBSN), and the P factor of the USLE (USLE_P), for which the starting values assumed the ideal conditions. These were modified according to a decrease in soil protection, in order to represent the erosive effect of the agricultural practices.

In their studies, Betrie et al. (2011) and Biru and Kumar (2017) considered the SPCON parameter as one of the most decisive in the determination of the maximum concentration of the sediment transported downstream. Related to this, both the flow parameters and the sediment transport parameters were classified in order of decreasing sensitivity. The order of the parameters in this ranking was as expected, since the analysis of the sediment load data indicated that the amounts of sediment transported by the runoff are negligible during days

Table 3 Ranking of the most influential parameters in the simulation of sediment transport

Parameter	Rank	P Value	t-Stat	Initial range	Default value	Fitted value
CN2.mgt	1	0.00	3.35	0–100	74.0	0.15
SPCON.bsn	2	0.20	1.34	0.0001–0.01	0.0001	0.53
SLSUBBSN.hru	3	0.31	−1.06	10–150	15.0	152.11
ALPHA_BF.gw	4	0.40	0.87	0–1	0.48	1.02
GW_DELAY.gw	5	0.41	−0.84	0–500	31.0	701.93
SPEXP.bsn	6	0.43	0.81	1–1.5	1.00	1.33
USLE_P.mgt	7	0.46	0.77	0–1	1.00	1.23
GWQMN.gw	8	0.67	−0.44	0–5000	1000	−0.13

without precipitation. This suggests that there are no sources or processes in the main channel that cause significant sediment transport.

3.2 Calibration and Validation

The calibration of the SWAT model showed that its performance was improved, relative to its pre-calibration configuration. The hydrological parameters identified in the sensitivity analysis, and fitted in the simulations of the calibration stage, were later used to perform the simulation in the validation. In Table 4, the performance of the model - for the calibration and validation in the flow and sediment load modeling (monthly and annual) - is evaluated. These simulations show that the model is able to satisfactorily describe the hydrological conditions and erosion processes that take place in basins such as that of the Argos River (Table 4).

According to these results, the values of the NSE, PBIAS, and RSR indices were good in both phases (calibration and validation) of the monthly flow modeling (NSE = 0.62 and 0.70, RSR = 0.61 and 0.54, PBIAS = −20.60% and − 16.09%, respectively), and were acceptable for the monthly sediment load modeling (NSE = 0.52 and 0.58, RSR = 0.70 and 0.64, PBIAS = 10.65% and 15.20%, respectively). On this time scale, the estimation of both variables improved with validation. Regarding the modeling of the annual flow and sediment load, these indices showed a substantial improvement compared to the monthly simulations. In this case, contrarily to what happened in the monthly simulations, the RSR, NSE, d, and R^2 values estimated for the validation period showed a reduction in the quality of the fit when compared to those of the calibration. For the flow variable, values of 0.89, 0.32, and − 15.20% were obtained for NSE, RSR, and PBIAS, respectively, in the calibration stage, and values of 0.70, 0.53, and − 13.60%, respectively, were obtained in the validation. The contrast in the goodness of fit between the two simulation phases was somewhat lower for the estimation of sediment transport (NSE = 0.81, RSR = 0.42, and PBIAS = 4.81% during the calibration stage, compared to NSE = 0.73, RSR = 0.51, and PBIAS = 11.90% in the validation). In addition, on both a monthly and an annual scale, the estimation of the flow showed a better fit than the estimation of the sediment load, this difference being more evident in the case of the monthly simulation.

These differences in the evaluation statistics of the annual model may indicate an overfit in the values of the parameters of the calibration period, which occurs with some regularity in

Table 4 Evaluation of the performance of the SWAT model in the calibration and validation of the monthly and yearly runoff and sediment simulation

Statistic	Discharge				Sediment Load			
	Calibration		Validation		Calibration		Validation	
	Monthly	Yearly	Monthly	Yearly	Monthly	Yearly	Monthly	Yearly
d	0.90	0.97	0.93	0.92	0.82	0.94	0.87	0.93
R^2	0.70	0.95	0.79	0.85	0.52	0.83	0.63	0.86
NS	0.62	0.89	0.70	0.70	0.50	0.81	0.58	0.73
RSR	0.61	0.32	0.54	0.53	0.70	0.42	0.64	0.51
PBIAS %	−20.60	−15.20	−16.09	−13.60	10.65	4.81	15.20	11.9
RMSE	0.24	0.08	0.16	0.07	1275.11	5425.45	862.65	3309.40

spatially distributed hydrological models (Schoups et al. 2008); therefore, the validation may better represent the accuracy of the model in future predictions. The PBIAS results for the modeling of the monthly and annual flow indicated an overestimation of 20.60% and 15.20%, respectively, in the calibration, while in the validation the overestimation was 16.10% and 13.60%, respectively. Hence, this was the only index that indicated a better fit in the validation of the annual flow, together with the statistical RMSE. However, in the sediment modeling, underestimations were obtained: of 10.65% and 4.81%, respectively, in the calibration and of 15.20% and 11.90%, respectively, in the validation.

The dispersion graphs of the flow values (monthly and annual) and the sediment load (monthly and annual) are shown for the calibration and validation stages in Figs. 2 and 3.

Generally, the determination coefficients (R^2) showed a good or very good correlation between the simulated and observed values. Throughout the modeling process, the fit of the predicted values to the observed ones was slightly poorer in the case of the monthly flow. The fit of the simulated annual flow was excellent in the calibration ($R^2 = 0.95$) and good in the validation ($R^2 = 0.85$). However, the residual values obtained in this case tended to deviate, being above the line of fit, in the lower tail of the distribution. This overestimation of the annual flow (Fig. 2) is due to the changes in the permeability of the karstic relief of the basin according to the climatic conditions. This implies different types of hydrological response in the sub-basins that make up the upper watershed area of the Argos River, probably influenced by the degree of connection of the underground flow with the eventual surface runoff. On the
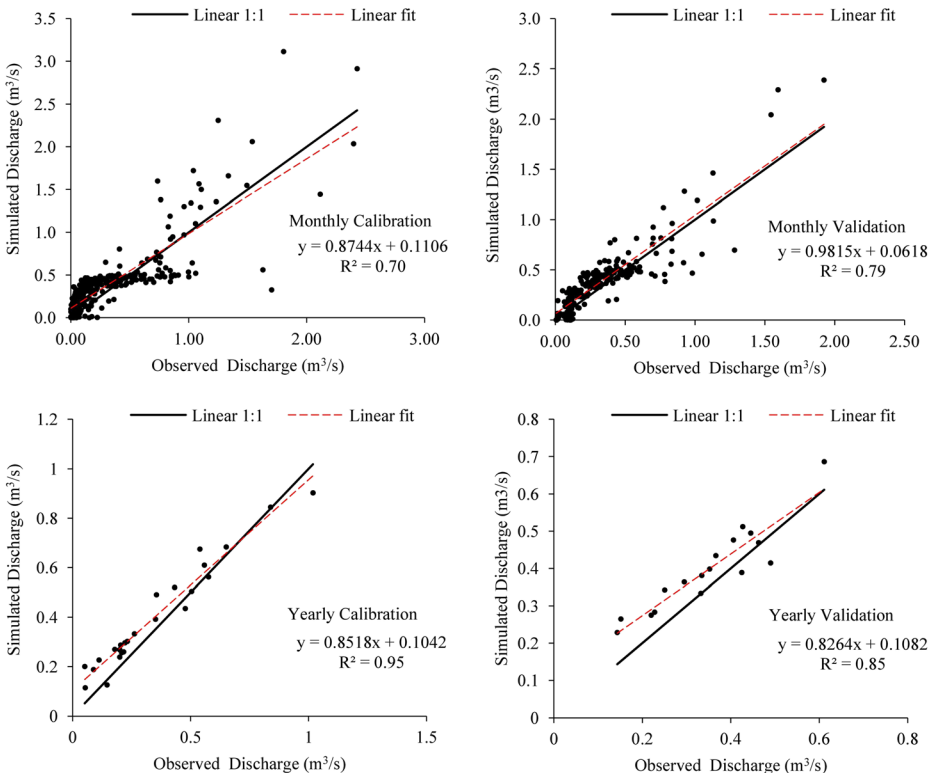

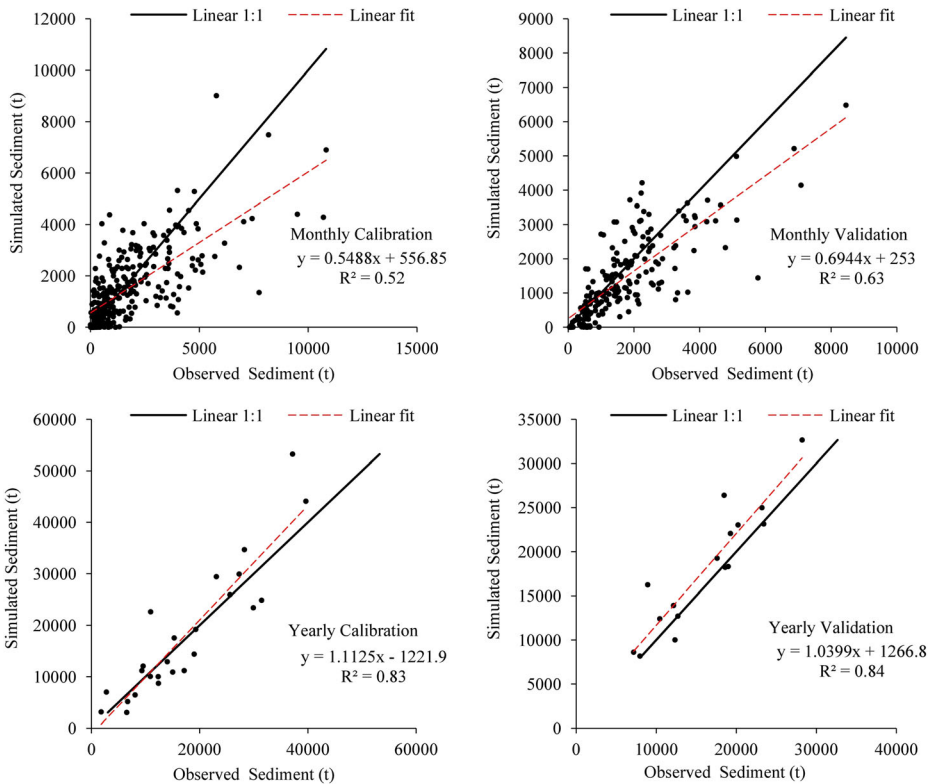**Fig. 2** Scattergrams of the monthly and yearly discharge

Fig. 3 Scattergrams of the monthly and yearly sediment load

other hand, an underestimation of the monthly sediment load can be observed, which seems to be due to the difficulty that the SWAT model has in simulating the effect of the hydrological events - that vary so much throughout the year (with low and extreme magnitude) - on the sediment transport, which would also explain its worse fit ($0.52 < R^2 < 0.63$). This effect disappears at the annual scale, for which there was a better fit of the predicted values ($R^2 = 0.84$). At this scale there was a slight overestimation of the transport that could be related to that of the annual flow, but, unlike the latter, the overestimation increased with the magnitude of the sediment load.

Figure 3 shows that the underestimation can be attributed to the fact that high-intensity, short-duration rainfall events often generate a sediment load that is greater than that simulated on the basis of monthly and annual rainfall data (Xu et al. 2009). These results are consistent with those obtained in previous studies (Baffaut and Benson 2009; Nerantzaki et al. 2015; Malagò et al. 2016; Briak et al. 2016; Chen et al. 2018), where the SWAT was tested to simulate the hydrological and erosive responses of watersheds with environmental conditions similar to ours.

In particular, Nerantzaki et al. (2015) evaluated the suspended sediment transport in a Mediterranean semiarid karst basin (on the island of Crete), using daily flow data and monthly sediment concentration data in the calibration of the SWAT model. The results showed a good fit and concordance between the measured and predicted values: values of NSE = 0.80, PBIAS = 25.30%, and RSR = 0.45 for the daily records and values of NSE = 0.83, PBIAS =

23.40%, and RSR = 0.41 for the monthly records were obtained during the validation. Briak et al. (2016) simulated the runoff volume and sediment concentration in the sexymiarid Kalaya basin (Northern Morocco) for the period 1971–1993. For the calibration (1976–1984) the fit was adequate for the flows (NSE and PBIAS = 0.76 and − 11.80%, respectively) and good for the concentration of sediment (NSE and PBIAS = 0.69 and 7.12%, respectively). During the validation period (1985–1993) the values of NSE and PBIAS were 0.67 and − 14.44%, respectively, for the flow and 0.70 and 15.51%, respectively, for the sediment load, which also shows a good fit of the model.

Outside the Mediterranean area, Molina-Navarro et al. (2014) studied the management of water resources in the semiarid basin of the Guadalupe River (Mexico)geuhThey evaluated several climate change scenarios based on water availability, obtaining satisfactory NSE values (the daily and monthly NSE values were, respectively, 0.66 and 0.86 for the calibration, and 0.52 and 0.76 in the validation). Yesuf et al. (2015) applied the SWAT to a basin in Ethiopia (Maybar) to quantify the sediment load at the outlet of the basin, and also reached satisfactory values of NSE (0.55 and 0.53), PBIAS (−14.6% and 0.8%), and RSR (0.67 and 0.69) for the calibration and validation, respectively.

Figures 4, 5, and 6 show the monthly and annual distribution of the observed and simulated discharge and sediment load. They also represent the series of monthly and annual rainfall, which allow analysis of the degree of relationship between the peaks of water flow and sediment transport and the maximum values of precipitation.

Figures 4 and 6a show how the hydrograph simulated for the monthly and annual discharge represents in a very satisfactory way the hydrological pattern observed for both stages of the
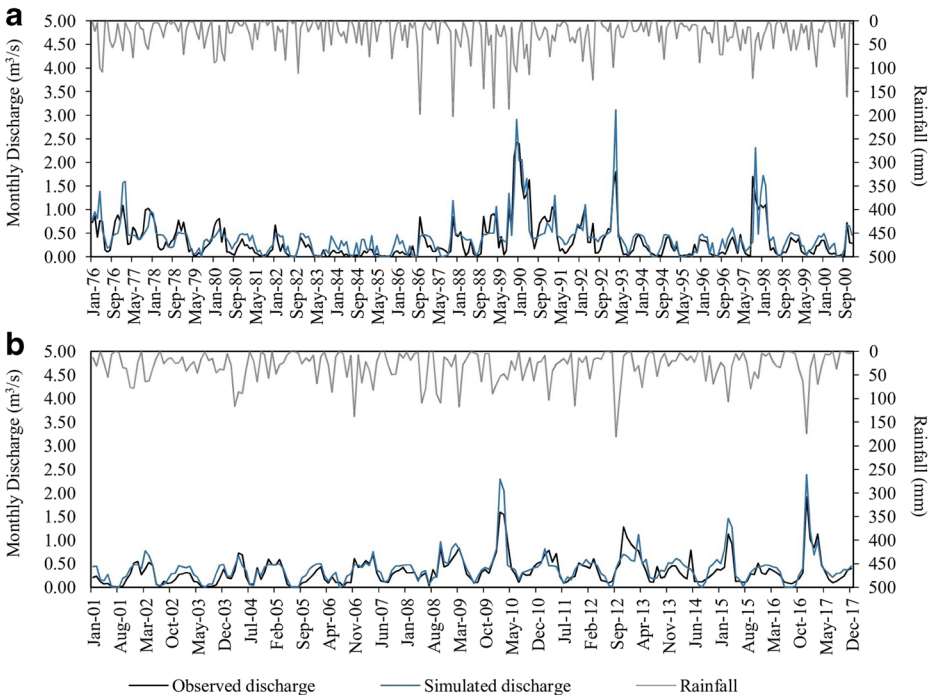

Fig. 4 Monthly discharge during the calibration period (1976–2000) (**a**) and the validation period (2001–2017) (**b**)
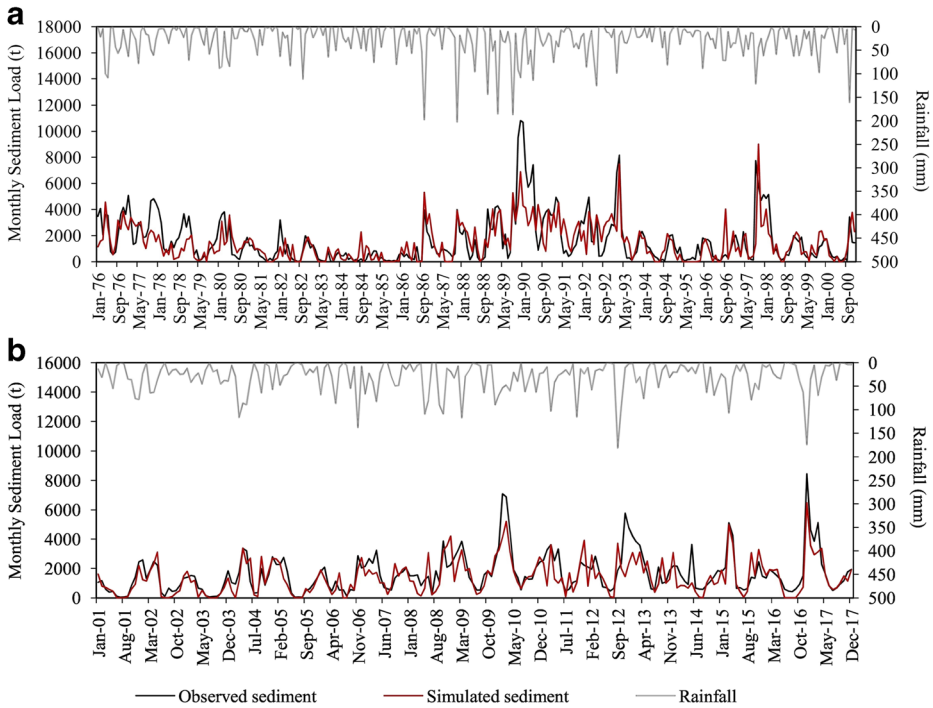
Fig. 5 Monthly sediment load during the calibration period (1976–2000) (**a**) and the validation period (2001–2017) (**b**)

modeling. With the exception of the most extreme values (maximum and minimum), the model fits quite well the series of discharge measured in the gauging stations. The calibration periods of Figs. 4a and 6a indicate that the predicted runoff was higher than the runoff observed in most years, with underestimations coinciding with relative maximums. The validation periods of Figs. 4b and 6a verify that the simulation tended to provide runoff values higher than those observed, except in the first years, when, as in the previous stage, the fit was worst at the points of maximum and minimum runoff.

The results from the flow modeling revealed the validity of this model for karstic basins, such as ours, in which the hydrological regulation exerted by the limestone formations of the headwater is especially noticeable on a monthly basis, as a consequence of the delay in the incorporation of underground flows and the damping of peak flows. Such results are consistent with those provided by Baffaut and Benson (2009), Yachtao (2009), Nikolaidis et al. (2013), and Wang and Brubaker (2014), in their implementations of SWAT models for basins with karstic regulation. It should be noted that Baffaut and Benson (2009) made a modification in the SWAT model to properly simulate the recharge of aquifers in a Missouri karst basin. Specifically, they modified the deep groundwater recharge equations by increasing the hydraulic conductivity in sinkholes that simulated ponds from which losses occurred in rivers. Yachtao (2009) included two new parameters for hydrological simulation and nitrate transport in aquifers. Nikolaidis et al. (2013) introduced five new parameters in order to improve the simulation of the karstic system and the recharge of the springs in the Koiliaris basin (Crete). More recently, Wang and Brubaker (2014) proposed a non-linear modification of the groundwater algorithm.
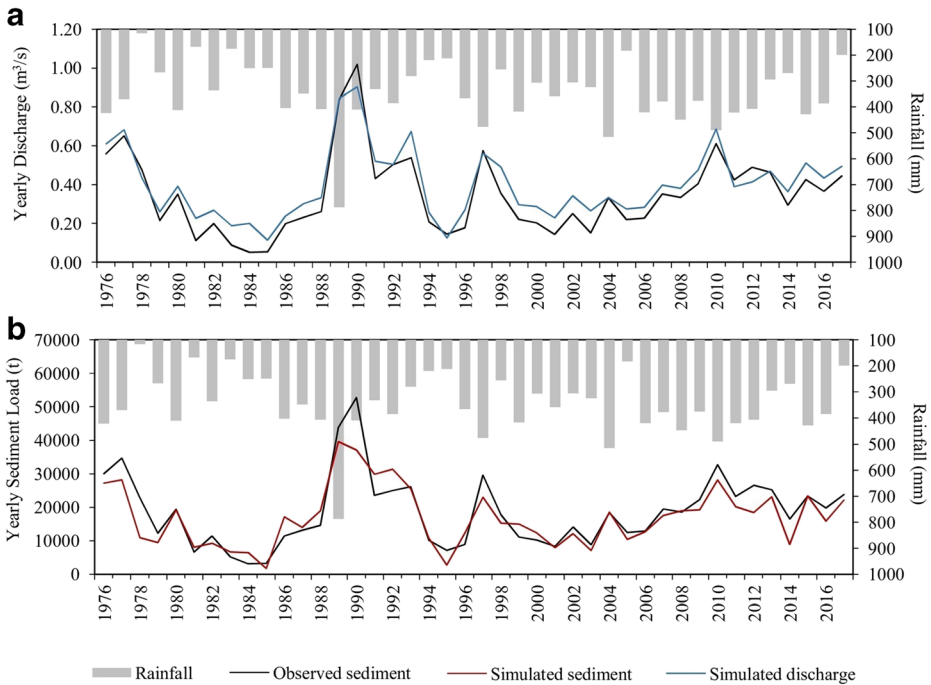
Fig. 6 Yearly discharge (**a**) and sediment load (**b**) during the calibration period (1976–2000) and the validation period (2001–2017)

The modeling of the sediment load (Figs. 5 and 6b) followed the tendency already described for the hydrological simulation: the agreement of the simulated and observed values was satisfactory for the monthly series and clearly improved for the annual series. As in the previous case, the fit was worst for the extreme values. Within the calibration period the simulation of the monthly and annual series offered a better fit in the stages of lower average discharge and sediment supply (e.g., 1979–1988 and 1993–1996) (Figs. 5a and 6b), and some underestimation of the solid load during the rest of this period. In contrast, during the validation (Figs. 5b and 6b), the sediment load predicted by the model was lower than that observed in most years. This could be due, in the opinion of several authors (Ghidey et al. 1995; Nearing 1998), to the occurrence of extreme events in the simulation period. The model reproduced more satisfactorily the sediment load in the first years of the series (2001–2010), with a more irregular fit at the end of the validation step.

The trend of the simulated sediment load coincided with that of the series of flow estimated by the model. Thus, the SWAT model tended to simulate higher sediment yield in the years with higher flow rates and to predict lower sediment supply in the years of lower simulated discharge.

As previously mentioned, it seems that the most difficult thing for the SWAT to do is model extreme values. Hence, the model estimated correctly the maximum sediment load of the validation period, for the year when the maximum sediment transport was observed (2010), but during the calibration period (Figs. 5a and 6b) the maximum sediment load estimated by the SWAT did not coincide with the year of highest estimated flow (1990), but was predicted for the previous year (1989).

For the absolute minimums, the behavior was more irregular, since in the calibration the minimum flow was estimated for the year 1995 and the minimum sediment load for 1985, while in the validation period the minimum simulated flow was for 2005 and the minimum simulated sediment production rate for 2003. Borah and Hart (1999), Biru and Kumar (2017), and Santos et al. (2018), compared the hydrographs and sedimentograms obtained with the SWAT and demonstrated the limitations of the SWAT in the evaluation of monthly maximum discharge and sediment load (which, in the main, were underestimated). Therefore, the simulations of storm events by the SWAT need to be improved, to achieve better prediction of sediment production in periods containing isolated flood peaks and occasional extreme events (e.g., flash floods).

4 Conclusions

The SWAT model has proved to be a good instrument for the estimation of flow and sediment transport in a semiarid Mediterranean basin with karst hydrological regulation at the headwater. The results of the present study, with regard to headwater streams in this type of basin (the volumes of surface runoff per channel, average annual flow, sedimentary contribution of each stream to the reservoir, annual sediment load, and material release ratio), can also be considered significant. As the sensitivity analyses have shown, this information obtained for the Upper Argos River is consistent with that provided by long series of flow gauging and sediment transport data in its reservoir. However, in both the calibration and the validation, the simulation by the SWAT was better for the flow rates than for the sediment load. Also, in both cases, the fit of the estimated annual values was better than that of the monthly ones. In fact, the stages when the karst influenced the hydrological regime do not fit the monthly scale, which could explain why the monthly values estimated by the SWAT were lower than the observed values. Throughout the modeling process, the fit of the predicted discharge to that observed was slightly worse in the case of the monthly values. The fit of the simulated annual discharge was excellent in the calibration ($R^2 = 0.95$) and quite significant in the validation ($R^2 = 0.85$). However, the residual values in this case tended to deviate, above the fit line, in the lower tail of the distribution. This implies different types of hydrological response in the sub-basins that make up the Upper Argos River area, probably influenced by the degree of connection of the groundwater system with sporadic torrential stream flows.

Regarding the sediment transport, the annual simulation also gave better results, since on this time scale the effect of the singular sedimentary contributions in times of heavy rain is cushioned. In contrast, the monthly simulation of the sedimentary load by the SWAT seems to still require modifications, including improvements in the estimation of the dissolved and suspended sediment load transported during heavy storms and flash flood events.

The use of long series of records during the calibration and validation processes and the breadth of the information at the basin level confer great reliability on the results obtained here and guarantee their applicability to basins with similar environmental conditions and lacking flow measurement stations and sediment transport data.

The results obtained are very useful for the prediction of information essential to the planning, implementation, and monitoring of soil conservation programs and water resources management in the study area and in other catchments of the Segura River Basin with similar environmental conditions. In addition, this work will allow the study of different scenarios of climate change and how these will affect the hydrological regimes of semiarid basins with karst hydrological regulation, which are highly vulnerable to this global problem.

Compliance with Ethical Standards

Conflict of Interest None.

References

Ahn S, Abudu S, Sheng Z, Mirchi (2018) A hydrologic impacts of drought-adaptive agricultural water management in a semi-arid river basin: case of Rincon valley, New Mexico. Agric Water Manag 209: 206–218

Arabi M, Frankenberger JA, Engel BA, Arnold JG (2008) Representation of agricultural conservation practices with SWAT. Hydrol Process 22:3042–3055

Arnold JG, Srinivasan R, Muttiah RS, Williams JR (1998) Large area hydrologic modeling and assessment part I: model development. J Am Water Resour Assoc 34(1):73–89

Arnold JG, Kiniry JR, Srinivasan R, Williams JR, Haney EB, Neitsch SL (2011) Soil and water assessment tool input/output file documentation, version 2009. Temple, Texas Water Resources Institute

Asl-Rousta B, Mousavi SJ, Ehtiat M (2018) SWAT-based hydrological Modelling using model selection criteria. Water Resour Manag 32:2181–2197

Baffaut C, Benson VW (2009) Modeling flow and pollutant transport in a karst watershed with SWAT. T ASABE 52:469–470

Betrie GD, Mohamed YA, Van Griensven A, Srinivasan R (2011) Sediment management modelling in the Blue Nile Basin using SWAT model. Hydrol Earth Syst Sci 15:807–818

Biru Z, Kumar D (2017) Calibration and validation of SWAT model using stream flow and sediment load for mojo watershed, Ethiopia. Sustain Water Resour Manag 4:937–949

Borah DK, Hart BT (1999) Frequency-selective fading channel estimation with a polynomial time-varying channel model. IEEE Trans Commun 47(6):862–873

Briak H, Moussadek R, Aboumaria K, Mrabet R (2016) Assessing sediment yield in Kalaya gauged watershed (northern Morocco) using GIS and SWAT model. J Soil Water Conserv 4:177–185

Brouziyne Y, Abouabdillah A, Bouabid R, Benaabidate L, Oueslati O (2017) SWAT manual calibration and parameters sensitivity analysis in a semiarid watershed in North-Western Morocco. Arab J Geosci 10:427–440

Brouziyne Y, Abouabdillah A, Bouabid R, Benaabidate L (2018) SWAT streamflow modeling for hydrological components' understanding within an agro-sylvo-pastoral watershed in Morocco. Journal of Materials and Environmental Sciences 9(1):128–138

CEDEX (Centro de Estudios Hidrográficos) (1994) Reconocimiento sedimentológico de embalses. Embalse de Argos. Madrid, Dirección General de Obras Hidráulicas

Chen Y, Chen X, Xu C, Zhang M, Liu M, Gao L (2018) Toward improved calibration of SWAT using season-based multi-objective optimization: a case study in the Jinjiang Basin in southeastern China. Water Resour Manag 32:1193–1207

Gassman PW, Reyes MR, Green CH, Arnold JG (2007) The soil and water assessment tool: historical development, applications, and future research directions. Trans ASAE 50:1211–1250

Ghidey F, Alberts EE, Kramer LA (1995) Comparison of runoff and soil loss predictions from the WEPP Hillslope model to measured values for eight cropping and management treatments. ASAE paper no. 95–2383. St. Joseph, American Society of Agricultural Engineers

Goyal MK, Panchariya VK, Sharma A, Singh V (2018) Comparative assessment of SWAT model performance in two distinct catchments under various DEM scenarios of varying resolution, sources and resampling methods. Water Resour Manag 32(2):805–825

Kiros G, Shetty A, Nandagiri L (2015) Performance evaluation of SWAT model for land use and land cover changes under different climatic conditions: a review. Hydrol Curr Res 6:216

Lin S, Jing C, Chaplot V, Yu X, Zhang Z, Moore N, Wu J (2010) Effect of DEM resolution on SWAT outputs of runoff, sediment and nutrients. Hydrol Earth Syst Sci 7:4411–4435

Luan XB, Wu PT, Sun SK, Li XL, Wang YB, Gao XR (2018) Impact of land use change on hydrologic processes in a large plain irrigation district. Water Resour Manag 32:3203–3217

Malagò A, Efstathiou D, Bouraoui F, Nikolaidis NP, Franchini M, Bidoglio G, Kritsotakis M (2016) Regional scale hydrologic modeling of a karst–dominant geomorphology: the case study of the island of Crete. J Hydrol 540:64–81

Martínez-Salvador A, Conesa-García C (2018) Estimation of suspended sediment and dissolved solid load in a Mediterranean semiarid karst stream using log-linear models. Hydrol Res 50(1):43–59

Molina-Navarro E, Martínez-Pérez S, Sastre-Merlín A, Bienes-Allas R (2014) Hydrologic modeling in a small Mediterranean basin as a tool to assess the feasibility of a Limno-reservoir. J Environ Qual 43(1):121–131

Moriasi DN, Arnold JG, Van-Liew MW, Bingner RL, Harmel RD, Veith TL (2007) Model evaluation guidelines for systematic quantification of accuracy in watershed simulations. T ASABE 50(3):885–900

Navarro-Hervas F, Rodríguez-Estrella T (2001) Desprendimientos y vuelcos en laderas, desencadenados por la sismicidad en la cuenca de Mula. In: Manero F (ed) Espacio natural y dinámicas territoriales: homenaje al Dr. Jesús García Fernández. Universidad de Valladolid, Valladolid, pp 171–182

Nearing MA (1998) Why soil erosion models over-predict small soil erosion losses and under-predict large soil losses. Catena 32:15–22

Neitsch SL, Arnold JG, Kiniry JR, Williams JR (2009) Soil and Water Assessment Tool Theoretical Documentation-Version 2009. Soil and water research laboratory. Temple, US Department of Agriculture - Agricultural Research Service

Nerantzaki SD, Giannakis GV, Efstathiou D, Nikolaidis NP, Sibetheros IA, Karatzas GP, Zacharias I (2015) Modeling suspended sediment transport and assessing the impacts of climate change in a karstic Mediterranean watershed. Sci Total Environ 538:288–297

Nikolaidis NP, Bouraoui F, Bidoglio G (2013) Hydrologic and geochemical modeling of a karstic Mediterranean watershed. J Hydrol 477:129–138

Santos CAS, Almeida C, Ramos TB, Rocha FA, Oliveira R, Neves R (2018) Using a hierarchical approach to calibrate SWAT and predict the semi-arid hydrologic regime of northeastern Brazil. Water 10(9):1137

Schmalz B, Fohrer N (2009) Comparing model sensitivities of different landscapes using the ecohydrological SWAT model. Adv Geosci 21:91–98

Schoups G, Van de Giesen NC, Savenije HHG (2008) Model complexity control for hydrologic prediction, water resources research, 44(12), W00B03

Wang Y, Brubaker K (2014) Implementing a nonlinear groundwater module in the soil and water assessment tool (SWAT). Hydrol Process 28(9):3388–3403

Williams JR, Brendt HD (1977) Sediment yield prediction based on watershed hydrology. Trans Am Soc Agric Eng 20:1100–1104

Xu ZX, Pang JP, Liu CM, Li JY (2009) Assessment of runoff and sediment yield in the Miyun reservoir catchment by using SWAT model. Hydrol Process 23(25):3619–3630

Yachtao GA (2009) Modification of the SWAT model to simulate hydrologic processes in a karst influenced watershed, (Master's thesis), Virginia-Tech, Department of Biosystems Engineering, Blacksburg

Yesuf HM, Assen M, Alamirew T, Melesse AM (2015) Modeling of sediment yield in Maybar gauged watershed using SWAT, Northeast Ethiopia. Catena 127:191–205

Yesuf HM, Melesse AM, Zeleke G, Alamirew T (2016) Streamflow prediction uncertainty analysis and verification of SWAT model in a tropical watershed. Environ Earth Sci 75:806

Yuan Y, Nie W, Sanders E (2014) Problems and prospects of SWAT model application on an arid/semi-arid watershed in Arizona. Conference, Reno, NV, March 23–27, 2014

Zettam A, Taleb A, Sauvage S, Boithias L, Belaidi N, Sánchez-Pérez JM (2017) Modelling hydrology and sediment transport in a semi-arid and Anthropized catchment using the SWAT model: the case of the Tafna River (Northwest Algeria). Water 9(3):216